Title
Performance of Nb3Sn Quadrupole Under High Stress

Author
Felice, H.

Publication Date
2012-05-18

Peer reviewed

Performance of a Nb_3Sn Quadrupole Under High Stress

H. Felice, B. Bingham, S. Caspi, D. Dietderich, P. Ferracin, A. Godeke, R. Hafalia, and G. L. Sabbi

Lawrence Berkeley National Laboratory, 1 Cyclotron Road, Berkeley CA 94720

M. Baijko, B. Bordini, L. Bottura, C. Giloux, A. Milanese, G. De Rijk and L. Rossi

CERN, CH-1211, Geneve, 23 Switzerland

This work was supported by the Director, Office of Science, Office of Fusion Energy Sciences, of the U.S. Department of Energy under Contract No. DE-AC02-05CH11231.

Performance of a Nb_3Sn Quadrupole Under High Stress

H. Felice, M. Bajko, B. Bingham, B. Bordini, L. Bottura, S. Caspi, G. De Rijk, D. Dietderich, P. Ferracin, C. Giloux, A. Godeke, R. Hafalia, A. Milanese, L. Rossi, and G. L. Sabbi

***Abstract*—Future upgrades of the Large Hadron Collider (LHC) will require large aperture and high gradient quadrupoles. Nb_3Sn is the most viable option for this application but is also known for its strain sensitivity. In high field magnets, with magnetic fields above 12 T, the Lorentz forces will generate mechanical stresses that may exceed 200 MPa in the windings. The existing measurements of critical current versus strain of Nb_3Sn strands or cables are not easily applicable to magnets. In order to investigate the impact of high mechanical stress on the quench performance, a series of tests was carried out within a LBNL/CERN collaboration using the magnet TQS03 (a LHC Accelerator Research Program (LARP) 1-meter long, 90-mm aperture Nb_3Sn quadrupole). The magnet was tested four times at CERN under various pre-stress conditions. The average mechanical compressive azimuthal pre-stress on the coil at 4.2 K ranged from 120 MPa to 200 MPa. This paper reports on the magnet performance during the four tests focusing on the relation between pre-stress conditions and the training plateau.**

***Index Terms*—Current cycling, high mechanical stress, Nb_3Sn quadrupole.**

I. Introduction

BASED on numerous studies performed on the strain sensitivity of Nb_3Sn strands [1], it is widely considered that Nb_3Sn magnets performance is very sensitive to mechanical strain and stress. The stress value of 150 MPa in compression was commonly considered as a limit to ensure good performance of a magnet. Nevertheless, extrapolating the behavior of an embedded strand within an impregnated cable from a bare strand measurement is a delicate exercise. Moreover, it is difficult to know the strain state of each wire in the magnet. Some work on ANSYS simulation is ongoing at LBNL [2], [3] in an attempt to model and understand the strand behavior on a microscopic level as well as a macroscopic level. Part of the simulation effort includes some tests which were carried out in collaboration between LBNL and CERN using the LARP TQS03 magnet. As detailed in a large number of publications [4], [5], the Technology Quadrupole (TQ) is a 1-meter long Nb_3Sn 90 mm aperture quadrupole developed in the framework of the US LHC Accelerator Program (LARP). This program aims at demonstrating the Nb_3Sn technology for the Large Hadron Collider future upgrades such as the luminosity upgrade requiring large aperture and high gradient quadrupoles. Several TQ magnets have been assembled using a collar-based mechanical structure (TQC series) [4] and a shell-based mechanical structure (TQS series) [5]. The TQS03 magnet used the shell-based structure. The primary purpose of this series was to validate the performance of the OST RRP 108/127 strand [6] as detailed in [7]. In addition, the TQS03 goal was to perform tests under variable preload conditions. Four tests in total took place at CERN. The results are presented and summarized in this paper along with the ANSYS analysis describing the stress distribution in the magnet. In the last test the magnet underwent additional current cycling. The magnet performance is reported here.

Manuscript received August 02, 2010; accepted October 20, 2010. Date of publication November 22, 2010; date of current version May 27, 2011. This work was partially supported by the Director, Office of Energy Research, Office of High Energy and Nuclear Physics, High Energy Physics Division, US Department of Energy, under Contract DE-AC02-05CH11231.

H. Felice, B. Bingham, S. Caspi, D. Dietderich, P. Ferracin, A. Godeke, R. Hafalia, and G. L. Sabbi are with the Lawrence Berkeley National Laboratory, Berkeley, CA 94720, USA (e-mail: hfelice@lbl.gov).

M. Bajko, B. Bordini, L. Bottura, C. Giloux, A. Milanese, G. De Rijk, and L. Rossi are with CERN, CH-1211, Geneve 23, Switzerland.

II. Magnet Design

A. Conductor

The conductor is a 0.7 mm diameter OST RRP 108/127 strand. The filament diameter is of the order of 50 microns. The critical current density is 2770 A/mm^2 at 12 T and 4.2 K, taking into account a self field correction of 0.585 T/kA. The TQ cable is made of 27 strands and is 10.06 $+/-$ 0.05 mm long and 1.26 $+/-$ 0.02 mm wide. The keystone angle is 1.05 $+/-$ 0.1 degree and the insulation thickness is 125 microns. This conductor has been demonstrated to be stable at 1.9 K [7].

B. Magnetic Cross-Section

TQ is a 1 meter long 90 mm aperture Nb_3Sn quadrupole made of four coils fabricated at FNAL (winding and curing) and LBNL (reaction and impregnation). Each coil is a double layer wound around a Titanium alloy pole (the cross-section is shown in Fig. 1). Table I summarizes the parameters of the TQS03 series.

III. Mechanical Behavior of the TQS03 Series

A. Mechanical Structure Analysis

The mechanical structure of TQS03 is a shell-based structure which relies on bladder and key technology to impart the preload to the coils [8] during assembly. The preload is transmitted to the coils by the loading keys. The bladders, made of two welded sheets of stainless steel, are inserted between the iron pads and the iron yokes (1018 steel) in each quadrant of the magnet (Fig. 2). During assembly, they are pressurized with water to create a clearance between the loading keys and

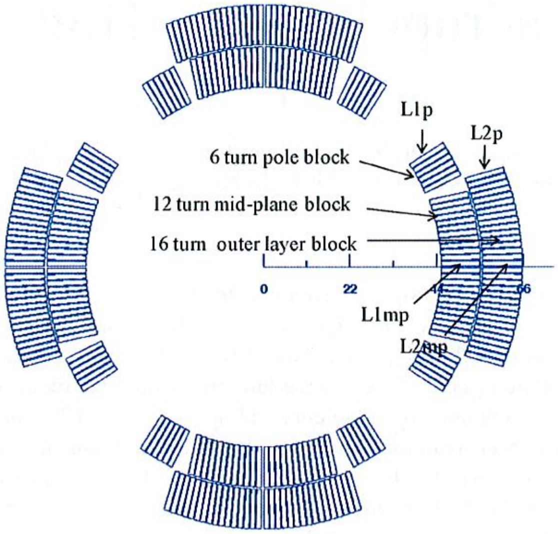

Fig. 1. TQ cross-section.

TABLE I
TQS03 PARAMETERS

	Units	TQS03
Short sample current at 4.3 K / 1.9 K	kA	13.2 / 14.5
Conductor peak field at 4.3 K / 1.9 K	T	11.96 / 13.02
Short sample gradient at 4.3 K / 1.9 K	T/m	234 / 254
Stored energy at 4.3 K / 1.9 K	kJ/m	433 / 522
Inductance	mH/m	5
Horiz. Lorentz force at 4.3 K per quad.	MN/m	1.9
Vert. Lorentz force at 4.3 K per quad.	MN/m	-2

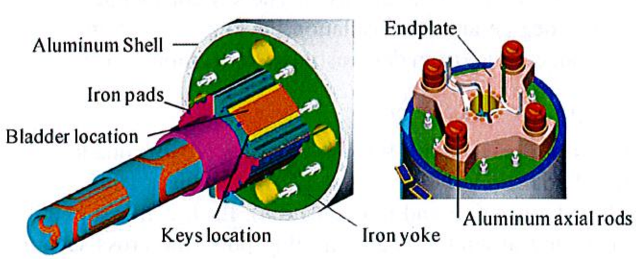

Fig. 2. TQS mechanical structure.

the yoke. The shimming of these keys maintains the pres-stress and allows the removal of the bladders. During cool-down, the differential thermal contraction between the 22 mm thick Aluminum alloy shell (7075 T6) and the iron yoke increases the shell tension and provides the additional azimuthal pre-load to the coils up to the target, usually the magnet short sample limit. The TQS structure also includes axial loading of the coils by means of four Aluminum rods connected to Stainless Steel endplates on both ends (Fig. 2). The rods are pre-tensioned at room temperature to a specific strain and their shrinkage during cool down provides additional axial preload to the coils via the endplates. The outer diameter of the TQS structure is 500 mm.

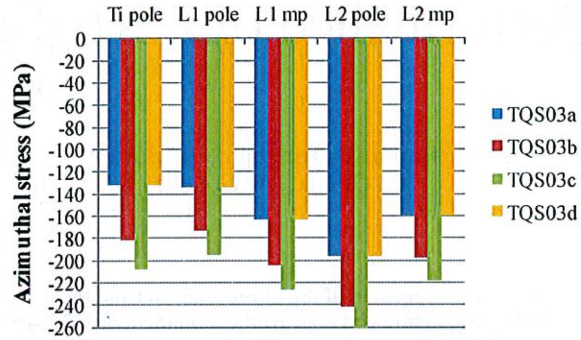

Fig. 3. Azimuthal stress in the coil after cool-down computed with ANSYS. L1, L2 correspond to the inner and the outer layer and L1pole (L2pole), L1mp (L2mp) correspond to the inner layer pole turn (outer layer pole turn) and the inner layer mid-plane turn (outer layer mid-plane turn).

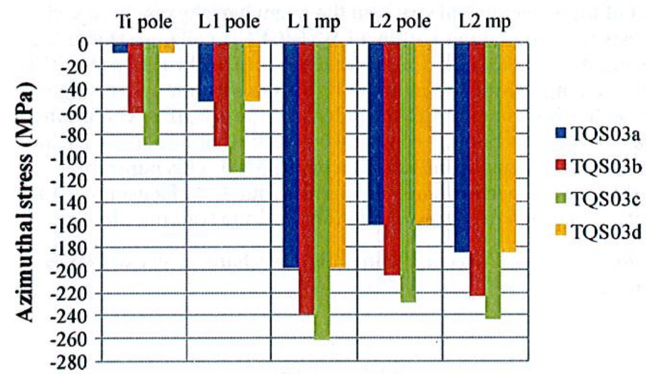

Fig. 4. Azimuthal stress in the coil with Lorentz forces at 12 kA computed with ANSYS.

In the TQS03 series, different loading conditions were studied. First, the TQS03a test was aimed at evaluating the performance of the new conductor. Therefore, the initial preload of the magnet was kept at minimum to avoid any conductor degradation due to stress. In contrast, the purpose of the TQS03b and TQS03c tests were to evaluate the impact of higher pre-stresses on the magnet performance. In TQS03d, the pre-stress was brought back to the TQS03a level to check for any permanent degradation. In all cases, a 3D ANSYS analysis was performed to guide the steps of the magnet assembly and to predict the stress state in the magnet after cool-down and during excitation. The ANSYS model included friction and contact elements between the different components of the magnet. The coil and the Titanium alloy pole piece were glued. Everywhere else, sliding with a 0.2 friction coefficient was considered. After bladder operation, the azimuthal pres-stress in the Ti pole is of the order of 50 MPa (respectively 90 MPa and 125 MPa) for TQS03a/d, respectively TQS03b and TQS03c. The pres-stress increases during cool-down. Fig. 3 summarizes the average stress in the coil predicted by the model after cool-down in the different magnets. From TQS03a to TQS03b and TQS03c, the average stress increased by step of ~40 MPa. As shown in Fig. 6, the axial preload is similar in each magnet.

Fig. 4 summarizes the ANSYS azimuthal stress in the coil with Lorentz forces. During excitation the pole turn is unloaded while the stress on the mid-plane increases. In all cases, the

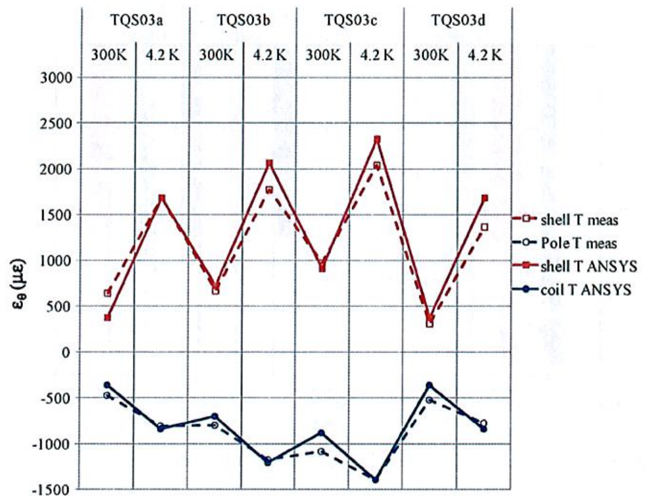

Fig. 5. Azimuthal strain variation in the coil Ti-alloy pole and in the Aluminum alloy shell: comparison between ANSYS computation and measurements. The points are measured or computed values. The lines are only a guide to the eye.

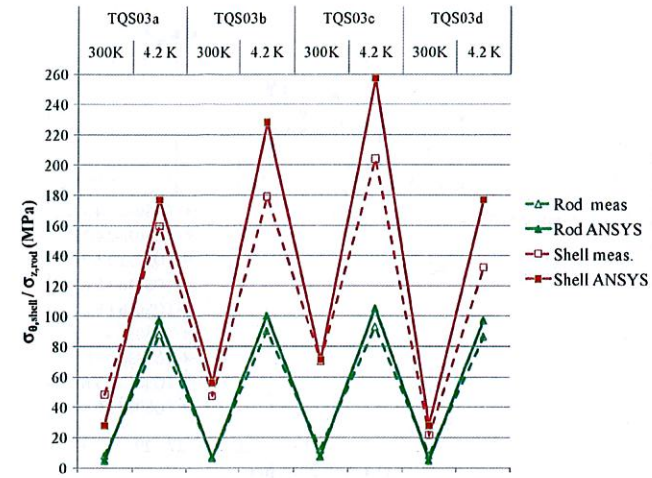

Fig. 6. Stress variation in the Al alloy shell (azimuthal) and in the rod (axial): comparison between ANSYS computation and measurements.

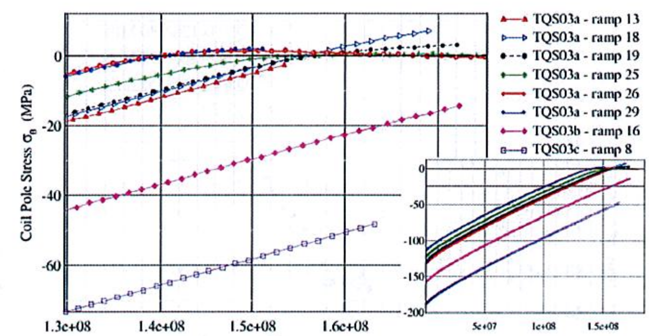

Fig. 7. Pole azimuthal stress versus square of the magnet current in A^2. The main graph shows the stress variation measured at high current. The insert is a zoom out of the same data.

stress in the layer 1 mid-plane turn is predicted to be equal or larger than 200 MPa.

B. *Mechanical Behavior During Assembly and Cool-Down*

The coil Ti alloy pole pieces are equipped with azimuthal and axial strain gauges. Additional strain gauges are mounted on the Aluminum alloy shell and on the Aluminum alloy rods as well. During assembly, the gauges are used to control the amount of preload applied to the coils and during cool-down, they confirm the strain state of the magnet. Fig. 5 shows the variation of azimuthal strain in the shell and in the pole after bladder operation (300 K) and cool-down (4.2 K). The good correlation between the measurements and the ANSYS computation can be seen.

It can also be noticed that with the same load key shimming, the strain in the pole after cool-down is slightly lower in TQS03a than in TQS03d. This can be explained by the fact that in TQS03a, the coils were virgin and underwent their first mechanical assembly removing all the fluffiness in the system. Therefore, with the same size of loading shims, the pre-stress in TQS03d is slightly lower after cool-down.

In Fig. 6, the measured stress (computed from measured strains) is compared to the ANSYS predicted azimuthal stress for the shell and axial stress for the rods. A small discrepancy can be observed between the shell stress measurements at 4.2 K and the ANSYS predicted stress. This can be explained by a difference between the ANSYS predicted axial strain of the shell and the measurements.

C. *Mechanical Behavior During Excitation*

During excitation, the strain measurements were performed and plotted with respect to the square of the magnet current (which is proportional to the Lorentz forces in the magnet). The data exhibit a linear azimuthal unloading of the pole piece. Due to the intentional low initial pre-stress applied in TQS03a [7], the preload was insufficient to keep the pole turn in contact with the pole piece. The appearance of a knee in the plot stress versus square of the current indicates a tendency of the pole turn to separate from the pole piece, tearing apart the epoxy bonding the pole turn to the pole. This can be seen in Fig. 7, where after several ramps, the azimuthal stress in TQS03a Ti pole becomes zero and remains flat.

In TQS03b and c, the preload was increased and the behavior remains linear during all the ramps.

IV. Quench Performance

A. *Training at 4.3 K*

As described in [7] and shown in Figs. 8 and 9, TQS03a was first trained at 4.3 K. The first quench reached 79% of the estimated short sample I_{ss}. After 3 quenches (referred as TQS03a-1 in Fig. 8), a resistance was detected in the splice between the magnet and the current lead. The magnet was warmed up and the splice repaired. On the second cool-down, the magnet had a first quench (quench #4 in Fig. 8) at 91% of its estimated short sample. Nine additional quenches followed reaching a stable plateau at 93% of I_{ss} which corresponds to a gradient of 220 T/m. With some additional preloading, TQS03b exhibited good memory by reaching a stable plateau in 2 quenches at 91% of its short sample. From this test on, the magnets did not show any training and reached stable plateaus right away. TQS03c and

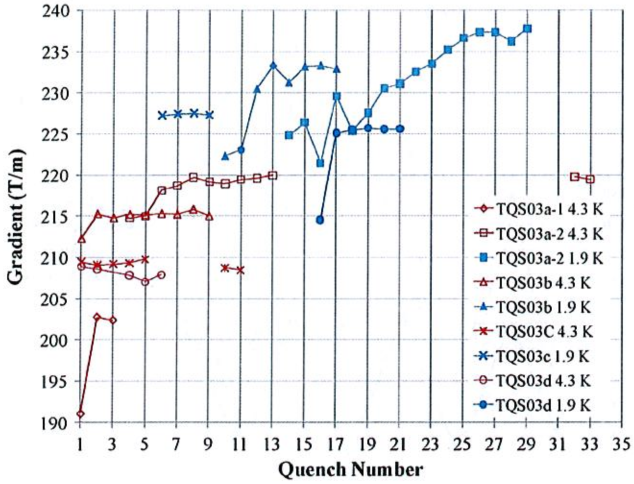

Fig. 8. Training performance summary of TQS03a, b, c, and d.

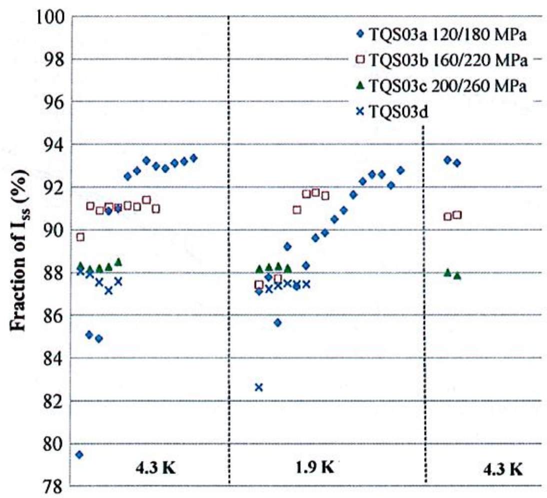

Fig. 9. Azimuthal strain variation in the coil Ti-alloy pole and in the Aluminum alloy shell.

TQS03d reached both 88% of the estimated short sample at the first quench.

B. Training at 1.9 K

One of the first goals of TQS03a was to demonstrate the stable behavior of the OST RRP 108/127 conductor at 1.9 K compared to the OST RRP 54/61 conductor used in the previous TQ magnets [7]. The test of TQS03a performed at 1.9 K showed a stable behavior. As shown in Fig. 9, the magnet continued to train reaching 93% of its calculated short sample at 1.9 K which corresponds to a gradient of 238 T/m. The magnet was still showing some sign of training when the test was stopped due to the unloading of the pole described in Part III. An increase of the preload was required to avoid damaging the coils. From TQS03b to TQS03d, the magnets behaved at 1.9 K in total agreement with its 4.2 K behavior, reaching 91% and 88% of its short sample. All the plateau quenches (at 4.2 K as well as 1.9 K) occurred in the mid-plane block of the inner and outer layer where the mechanical stress is the highest (260 MPa in

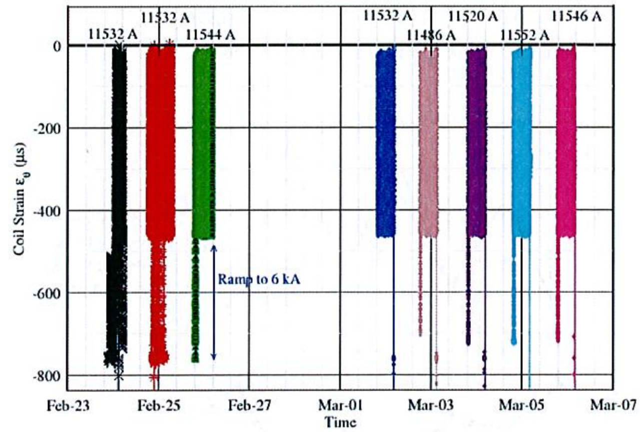

Fig. 10. Summary of TQS03d cycling: azimuthal strain versus time.

TQS03c). The test of TQS03d showed that the degradation of the plateau observed in TQS03c was permanent. Nevertheless, it is important to note that this degradation is minimal (only 5%) with respect to the stress level reached in the coil (260 MPa in TQS03c).

V. Cycling

The main goal of the test of TQS03d was to check the permanent nature of the plateau reduction. The secondary purpose of this test was to test the behavior of a Nb_3Sn magnet under current cycling conditions. During 8 days, the magnet was cycled with a triangular cycle of 50 A/s. With a stable training plateau around 11.5 kA, the upper bound of the cycle was kept at 11 kA. Due to high flux jump activity at low current, the detection thresholds had to be increased at low currents. The change of threshold, being done manually, prevented reducing the lower bound below 6 kA and permitted a constant voltage detection threshold during the cycle. The first 2 days, 35 and 106 cycles were performed in order to set up the system. During the following days, 145 cycles were carried out daily. At the end of each day, after the 145 cycles, the magnet was quenched to check for any degradation. The quench current is listed in Fig. 10 above each series of cycles. In total, the magnet was cycled 1000 times and did not show any signs of plateau degradation. As seen in Fig. 10, the strain state of the coil remained constant during the cycles.

VI. Conclusion

The TQS03 series of tests was used to investigate the impact of high pre-stress on the magnet performance and showed that despite a very high mechanical stress in the winding (up to 260 MPa), the magnet experienced very little degradation. After each thermal cycle and increase of preload, the magnet did not experience any retraining reaching the plateau right away. Finally, the magnet responded well to the current cycling with no strain degradation and no spontaneous quenches during cycling.

Acknowledgment

The authors thank the LBNL technical staff and the CERN assembly and testing groups who greatly contributed to the success of these tests.

REFERENCES

[1] A. Godeke *et al.*, "A general scaling relation for the critical current density in Nb_3Sn," *Supercond. Sci. and Technol.*, vol. 19, pp. R100–R106, 2006.

[2] B. Collins *et al.*, Introduction of Nonlinear Properties Into Hierarchical Models of Nb_3Sn Strands this proceedings.

[3] D. Arbelaez *et al.*, "Cable deformation simulation and a hierarchical framework for Nb_3Sn Rutherford cables," *J. Phys.: Conf. Ser.*, vol. 234, 2010.

[4] S. Feher *et al.*, "Development and test of LARP Technological Quadrupole (TQC) magnet," *IEEE Trans. Applied Supercond.*, vol. 17, no. 2, pp. 1126–1129, June 2007.

[5] S. Caspi *et al.*, "Test and analysis of Technology Quadrupole Shell (TQS) magnet models for LARP," *IEEE Trans. Applied Supercond.*, vol. 18, no. 2, pp. 179–183, June 2008.

[6] J. A. Parrell *et al.*, "High field Nb_3Sn conductor development at Oxford Superconducting Technology," *IEEE Trans. Appl. Supercond.*, vol. 13, no. 2, 2003.

[7] H. Felice *et al.*, "Test results of TQS03: A LARP shell-based Nb_3Sn quadrupole using 108/127 conductor," *J. Phys.: Conf. Ser.*, vol. 234, 2010.

[8] S. Caspi *et al.*, "The use of pressurized bladders for stress control of superconducting magnets," *IEEE Trans. Appl. Supercond.*, vol. 11, no. 1, June 2001.